

Meta-transition between an inverted BKT transition and an abrupt transition in the bond percolation on a random hierarchical small-world network

Tomoaki Nogawa*

Faculty of Medicine, Toho University, 5-21-16, Omori-Nishi, Ota-ku, Tokyo 143-8540, Japan

Takehisa Hasegawa†

*Graduate School of Information Science, Tohoku University,
6-3-09, Aramaki-Aza-Aoba, Sendai, Miyagi 980-8579, Japan*

(Dated: December 10, 2018)

We study bond percolation on a one-parameter family of hierarchical small-world network, and find a meta-transition between the inverted BKT transition and the abrupt transition driven by changing the network topology. It is found that the order parameter is continuous and fractal exponent is discontinuous in the inverted BKT transition, and oppositely, the former is discontinuous and the latter is continuous in the abrupt transition. The gaps of the order parameter and fractal exponent in each transition go to vanish as approaching the meta-transition point. This point corresponds to a marginal power-law transition. In the renormalization group formalism, this meta-transition corresponds to the transition between transcritical and saddle-node bifurcations of the fixed point via a pitchfork bifurcation.

Recently, cooperative phenomena, e.g. percolation and ferromagnetism, on various kind of non-Euclidean graphs have been extensively investigated in the context of complex networks, and a lot of exotic behaviors have been found [1]. One of the most remarkable facts is that such a system often exhibits a critical phase [2], inside which a system always shows properties typical for ordinary critical *points* of the second order transition such as infinite susceptibility and zero order parameter [3]. This phase lies between an ordered phase, (e.g., a percolating phase and a ferromagnetic phase) and a disordered phase (e.g., a non-percolating phase and a paramagnetic phase), but is not a boundary but occupies finite fraction of the parameter space. Although such a phase is similar to the quasi-long-range-order phase of the two-dimensional XY model, the origin is quite different. Some studies imply that a critical phase is attributed to a small-world property of graphs [3–5].

Recognition of a critical phase leads us to have interest on a transition between critical and noncritical phases. To our knowledge, the type of singularity for a disorder-critical transition is unique, which is observed in nonamenable graphs such as trees [2, 6, 7]. On the other hand, the singularity for a critical-order transition, which is the subject of this letter, are distinguished by the behavior of the order parameter near the phase boundary as: (T1) power-law transitions [5], (T2) inverted Berezinskii-Kosterlitz-Thouless (iBKT) transitions [3] and (T3) abrupt transitions [2, 8]. The order parameter m varies with the distance from the phase boundary ε in the ordered phase as $m \propto \varepsilon^\beta$ in T1, $m \propto \exp[-\alpha/\varepsilon^{1/2}]$ in T2, and $m = m_c + c_1\varepsilon^b$ in T3, respectively. Here $\beta, \alpha, m_c, c_1, b$ are constants.

On the other hand, singularity cannot be quantified by the ε -dependence of m or susceptibility χ in a critical phase where $m = 0$ and $\chi = \infty$ in infinite size systems.

The authors proposed a characterization of the singularity by the fractal exponent ψ [4]. It is related to the finite size dependence of a local disconnected susceptibility of a specific site $\tilde{\chi}$, which includes the contribution of the long-range coherence and corresponds to the size of the cluster containing the focused site in percolation models. On highly inhomogeneous graphs such as nonamenable graphs, where the boundary effect is not negligible even in the thermodynamic limit, and scale free networks, the local disconnected susceptibility of a central site or hub can diverge even though the spatially averaged susceptibility does not. Therefore the critical phase of such a system is characterized better by the former [2, 5, 8–11]. We introduce ψ such that $\tilde{\chi} \propto N^\psi$, where N is the number of degrees of freedom. While ψ takes trivial values: 0 in a disordered phase and 1 in an ordered phase, it takes a fractional value between 0 and 1 in a critical phase. Previous studies on several systems indicates that the continuity of ψ at a critical-order transition is opposite to that of m ; ψ continuously approaches 1 as $1-\psi \propto \varepsilon^\nu$ in T3 [2, 8] while it continuously approaches an edge value $\psi_c < 1$ from below and jumps to 1 in T1 and T2 [5].

At this moment, we lacks unified picture on various critical-order transitions. Recently, all of the aforementioned transitions were found in different models on the same graph, hierarchical small-world network (HSWN) with one-dimensional (1d) backbone, known as Farey graph [12]: T2 for the Q -state Potts model with $Q \geq 3$ [10], T1 for the Potts model with $Q = 2$ [11] and T3 for bond percolation [8]. Note that bond-percolation can be mapped to the Potts model with $Q = 1$. The authors predicted a meta-transition by changing Q at $Q_c = 2$ [11]. Here meta-transition means the transition between transitions T2 and T3 via T1 as a meta-transition point. Although this meta-transition can be a clue to establish comprehensive theory of the critical-order transitions, its

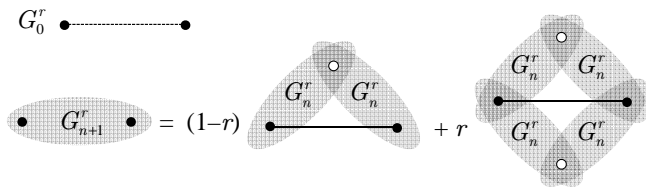


FIG. 1. Initial graph G_0^r and schematic diagram of the recursive construction of the hierarchical graph. The filled circles are roots of both G_n^r and G_{n+1}^r , and the empty circles are roots only of G_n^r and not of G_{n+1}^r . The solid and broken lines indicate backbone and shortcut edges, respectively.

property is rarely understood because the number of spin state Q , which is an integer, cannot be change continuously. In this letter, we analyze the meta-transition in detail by treating bond percolation on a random HSWN whose topology can be changed by a *continuous* parameter.

Structure of Graph : Here we explain how to construct the sequence of random graphs that we treat. We start with G_0^r that consists of two vertices, which are called “roots”, connected by a “backbone edge”. As illustrated in Fig. 1, we recursively make a graph G_{n+1}^r from two G_n^r 's with probability $1-r$, and from four G_n^r 's with probability r . Here G_n^r 's are independent random realizations. In both cases, we make graph-operations: joining pairs of root vertices in G_n^r 's to be one vertex, letting the two of the roots in G_n^r 's be the roots of G_{n+1}^r , and adding a “shortcut edge” connecting the new roots. The deterministic cases with $r=0$ and $r=1$ coincide with a Farey graph [8, 10, 11] and the decorated (2,2)-flower [3, 5, 13, 14], respectively. The expectation value of the number of vertices in G_n^r increases as

$$\langle N_{n+1} \rangle = \langle k \langle N_n \rangle - l \rangle, \quad (1)$$

where $\langle \dots \rangle$ means average over graph realization. Random variable (k, l) equal (2,1) with probability $1-r$ and (4,4) with probability r . Then we have $\langle N_n \rangle = [(1+r)\kappa^n + (1+3r)]/(1+2r)$, and $\langle N_n \rangle$ is approximately proportional to $\kappa(r)^n$ for $n \gg 1$, where $\kappa(r) \equiv 2(1+r)$. We call the subgraph obtained by removing all shortcut edges a backbone, where the shortest path length between the two roots equals $L_n = 2^n$. The effective dimension of the backbone d_{eff} such that $\langle N_n \rangle \propto (L_n)^{d_{\text{eff}}}$ is given by $d_{\text{eff}} = \log_2 \kappa(r)$, which monotonically changes $1 \rightarrow 2$ with $r: 0 \rightarrow 1$. With the shortcut edges, the graph is infinite-dimensional in the sense that the shortest path length is proportional to $\ln N_n$.

Renormalization of percolating probability: We consider bond percolation on G_n^r . Let the open-bond probability be p for both backbone and shortcut edges. By utilizing the hierarchical structure of G_n^r , we can derive an exact renormalization group (RG) map of p . We introduce the probability p_n that the two roots of G_n^r are connected,

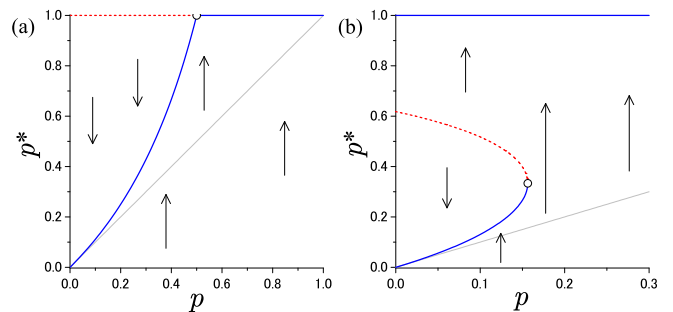


FIG. 2. (Color online) Renormalization group flow diagram for (a) $r=0$ and (b) $r=1$. The solid (blue) and broken (red) lines denote stable and unstable fixed points, respectively. The thin gray lines indicate $p^* = p$, which is the starting points of the RG flow.

i.e., they belong to the same cluster. Its average over graph realization satisfies the recursion equation starting from $p_0 = p$:

$$p_{n+1} = 1 - (1-p)(1-p_n^2)(1-rp_n^2), \\ \Leftrightarrow p_{n+1} - p_n = (1-p_n)[p(1+A(r,p_n)) - A(r,p_n)], \quad (2)$$

where $A(r,p) \equiv p[1-rp(1+p)]$. Hereafter, p_n denotes an averaged value over graph realizations. The nontrivial fixed point (NTFP) for given r and p , $p^*(r,p) \in (0,1)$, is obtained by solving

$$A(r,p^*) = p/(1-p). \quad (3)$$

Figure 2(a) shows the RG flow for the case of $r=0$ (Farey graph). We consider the flow starts at $p_0 = p$. As p increases, a transcritical bifurcation of the stable fixed point occurs at $p = p_c = 1/2$; p_n converges to the NTFP for $p < p_c$ and to 1 for $p > p_c$. Thus the system is in a critical phase for $p < p_c$ and in a percolating phase for $p > p_c$. There does not exist a nonpercolating phase corresponding to $p^* = 0$. The above bifurcation corresponds to T2 as shown in Ref. [8].

For the case of $r=1$ (decorated (2,2)-flower), there exist two NTFPs for $p < p_{\text{sn}}^* = 5/32$ as shown in Fig. 2(b). The one with smaller p^* is stable and another is unstable. The two NTFPs meet and annihilate together at the saddle-node bifurcation point (SNBP), $(p, p^*) = (p_{\text{sn}}, p_{\text{sn}}^*) = (5/32, 1/3)$. Consequently, a saddle-node bifurcation occurs with increasing p ; p_n converges to the stable NTFP for $p < p_c = p_{\text{sn}}^*$ and to 1 for $p > p_c$. Therefore p^* jumps from p_{sn}^* to $p^* = 1$. This bifurcation corresponds to T3 as shown in Ref. [5, 14]. (Note that the stable fixed point $p^* = 1$ and the unstable fixed point for $p < p_c$ are irrelevant in the present case with $p_0 = p < p^*(r,p)$.)

Next we consider the case of general $r \in [0,1]$. Figure 3(a) shows the p -dependence of the NTFP for several r 's. Types of bifurcation of the RG fixed point changes at $r = r_c = 1/5$; saddle-node type for $r > r_c$ and transcritical type for $r \leq r_c$. The SNBP is given by $\partial p / \partial p^* = 0$,

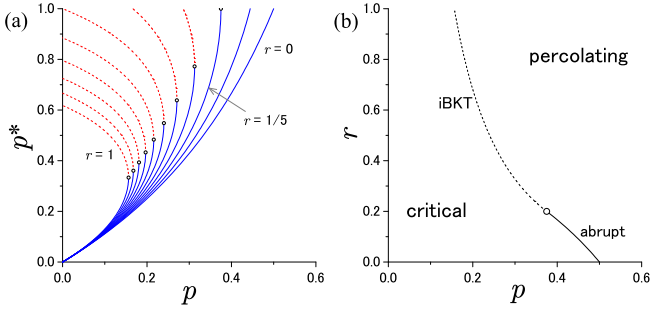


FIG. 3. (Color online) (a) p -dependence of the nontrivial fixed points for $r = 0.0 - 1.0$ (0.1 step). The solid (blue) and broken (red) lines denote stable and unstable fixed points, respectively. (b) phase diagram in the $r \times p$ plane. Abrupt transition occurs across the solid line and iBKT transition does across the broken line.

which leads to

$$(p_{\text{sn}}(r), p_{\text{sn}}^*(r)) = \left(\frac{A(r, p_{\text{sn}}^*(r))}{1 + A(r, p_{\text{sn}}^*(r))}, \frac{\sqrt{1 + 3/r} - 1}{3} \right) \quad (4)$$

As r decreases, p_{sn}^* becomes larger to be unity at $r = r_c$, and the SNBP enters the unphysical region $p^* > 1$. At $r = r_c$, a pitchfork bifurcation occurs by changing p . Equation (3) leads to the p -dependence of the *stable* fixed points near and below p_c for given r as

$$1 - p^*(r, p) = \begin{cases} |\varepsilon| & \text{for } r < r_c \\ \sqrt{|\varepsilon|} & \text{for } r = r_c \\ [1 - p_{\text{sn}}^*(r)] + \sqrt{|\varepsilon|} & \text{for } r > r_c \end{cases} \quad (5)$$

Here $\varepsilon \equiv p - p_c(r)$ and we omit unimportant coefficients of power of $|\varepsilon|$ [same as in Eqs. (11) and (14) appearing later]. In the limit $r \rightarrow r_c + 0$, the gap of p^* at p_c , i.e. $1 - p_{\text{sn}}^*$, continuously approaches 0 as

$$1 - p_{\text{sn}}^*(r) = (25/8)(r - r_c) + O((r - r_c)^2). \quad (6)$$

Figure. 3(b) shows the phase diagram in the $r \times p$ plane. Threshold probability $p_c(r)$ is given by $p_{\text{sn}}(r)$ for $r > r_c$ and by $[1 + A^{-1}(r, 1)]^{-1}$ for $r < r_c$. As shown next, the point $(r_c, p_c(r_c))$ plays a similar role with a tricritical point, which joins a first-order transition boundary and a second-order one.

Generating function analysis: We investigate the order parameter and the fractal exponent of the root cluster, i.e., the cluster that one root belongs to. The mean size of the root cluster can be calculated by using the generating function $Z_n(x) = \sum_s z_{n,s} x^s$ where $z_{n,s}$ is the probability that a root belongs to a cluster with size s . We split it in two terms as $Z_n(x) = x^2 T_n(x) + x \bar{T}_n(x)$ with $T_n(x) = \sum_{s=0}^{\infty} t_{n,s} x^s$ and $\bar{T}_n(x) = \sum_{s=0}^{\infty} \bar{t}_{n,s} x^s$, where $t_{n,s}$ is the probability that a root belongs to a cluster with size $s+2$ that includes another root, and $\bar{t}_{n,s}$ is the probability that a root belongs to a cluster with size $s+1$ that does not

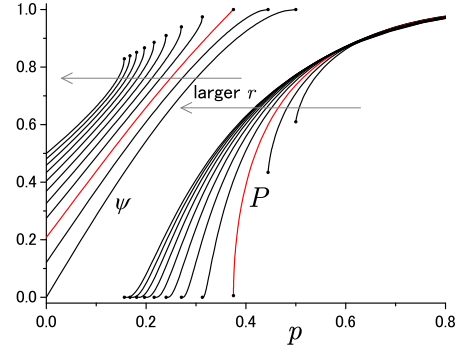


FIG. 4. (Color online) p -dependence of fractal exponent ψ for $p \leq p_c(r)$ and order parameter P for $p \geq p_c(r)$ for $r = 0.0 - 1.0$ (0.1 step). We show the numerical data with $n = 65536$ for P , in which finite size effect is negligible in this plot.

include another root [5]. The expectation value of a root cluster size is given by

$$s_n^{\text{rt}} = Z'_n(1) = [2T_n(1) + \bar{T}_n(1)] + [T'_n(1) + \bar{T}'_n(1)], \quad (7)$$

where the primes indicate the derivatives with respect to x , and $T_n(1) = 1 - \bar{T}_n(1) = p_n$. The recursion equations of $T'_n(1)$ and $\bar{T}'_n(1)$ for general r is obtained by utilizing those for $r = 0$ in Ref. [8], and for $r = 1$ in Ref. [5] as

$$\langle \bar{\tau}_{n+1} \rangle = \langle M_n \langle \bar{\tau}_n \rangle + \bar{c}_n \rangle, \quad \bar{\tau}_n \equiv \left(\frac{T'_n(1)}{\bar{T}'_n(1)} \right). \quad (8)$$

Here (M_n, \bar{c}_n) equals $(M_n^{(0)}, \bar{c}_n^{(0)})$ with probability $1 - r$ and $(M_n^{(1)}, \bar{c}_n^{(1)})$ with probability r where

$$\begin{aligned} M_n^{(0)} &= \begin{pmatrix} 2[\bar{p}p_n + p] & 2p\dot{p}_n \\ \bar{p}\bar{p}_n & \bar{p}\dot{p}_n \end{pmatrix}, \quad \bar{c}_n^{(0)} = \begin{pmatrix} p_n[p_n + 2p\bar{p}_n] \\ \bar{p}p_n\bar{p}_n \end{pmatrix}, \\ M_n^{(1)} &= \begin{pmatrix} 4[1 - \bar{p}\bar{p}_n^2\dot{p}_n] & 4\dot{p}_n[p_n^2 + p\bar{p}_n\dot{p}_n] \\ 2\bar{p}\bar{p}_n^2\dot{p}_n & 2\bar{p}\bar{p}_n\dot{p}_n^2 \end{pmatrix}, \\ \bar{c}_n^{(1)} &= \begin{pmatrix} 2p_n[2 - p_n - 2\bar{p}\bar{p}_n^2\dot{p}_n] \\ 2\bar{p}p_n\bar{p}_n^2\dot{p}_n \end{pmatrix}, \\ \bar{p} &\equiv 1 - p, \quad \bar{p}_n \equiv 1 - p_n, \quad \dot{p}_n \equiv 1 + p_n. \end{aligned} \quad (9)$$

First, we consider the singularities of the fractal exponent. We have $\langle s_n^{\text{rt}} \rangle \propto [\lambda(r, p^*)]^n$ for large n , where $\lambda(r, p)$ is the larger eigenvalue of $M_n^{(r)} = (1-r)M_n^{(0)} + rM_n^{(1)}$ with $p_n = p^*(r, p)$. Then the fractal exponent $\psi(r, p)$ such that $\langle s_n^{\text{rt}} \rangle \propto \langle N_n \rangle^{\psi(r, p)}$ is given as $\psi(r, p) = \ln \lambda(r, p) / \ln \kappa(r)$. The p -dependence of ψ for several values of r is shown in Fig. 4. For given r , ψ increases with p for $p < p_c(r)$, and equals 1 for $p > p_c(r)$. Near and below $p = p_c(r)$, we numerically found that $1 - \psi$ obeys to the power-law whose exponent depends on r as

$$1 - \psi(r, p) = \begin{cases} |\varepsilon|^2 & \text{for } r < r_c \\ |\varepsilon| & \text{for } r = r_c \\ [1 - \psi_c(r)] + \sqrt{|\varepsilon|} & \text{for } r > r_c \end{cases} \quad (11)$$

where $\psi_c(r) \equiv \psi(r, p_c(r))$.

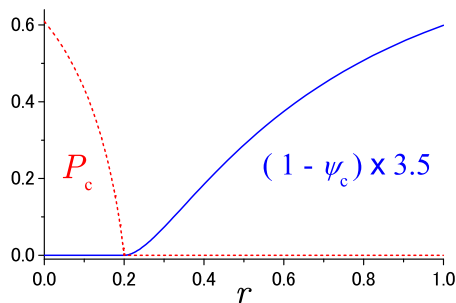


FIG. 5. (Color online) r -dependence of $1 - \psi_c$ (blue solid line) and P_c (red broken line).

Next, we consider the singularities of an order parameter $P \equiv \langle s_n^{\text{rt}}/N_n \rangle$. To calculate P , we solve recursion equations:

$$\left\langle \frac{\vec{\tau}_{n+1}}{N_{n+1}} \right\rangle = \left\langle \frac{M_n(N_n^{-1}\vec{\tau}_n) + N_n^{-1}\vec{c}_n}{k - lN_n^{-1}} \right\rangle \approx \left\langle \frac{M_n\langle N_n^{-1}\vec{\tau}_n \rangle + \langle N_n^{-1} \rangle \vec{c}_n}{k - l\langle N_n^{-1} \rangle} \right\rangle, \quad (12)$$

$$\langle N_{n+1}^{-1} \rangle = \left\langle \frac{N_n^{-1}}{k - lN_n^{-1}} \right\rangle \approx \left\langle \frac{\langle N_n^{-1} \rangle}{k - l\langle N_n^{-1} \rangle} \right\rangle. \quad (13)$$

In these formulae, we make an approximation to take the average of N_n^{-1} in the denominator in advance, which is good for large N_n . The p -dependence of P for $p > p_c(r)$ is shown in Fig. 4. While P for $n \rightarrow \infty$ equals 0 for $p < p_c$, P is finite and increases with p above p_c . Near and above $p_c(r)$, we numerically found three types of singular behavior for P depending on r as

$$P(r, p) = \begin{cases} P_c(r) + \varepsilon & \text{for } r < r_c \\ \varepsilon^\beta & \text{for } r = r_c \\ \exp[-\alpha(r)/\sqrt{\varepsilon}] & \text{for } r > r_c \end{cases}, \quad (14)$$

where $P_c(r) = P(r, p_c(r))$. We estimate $\beta = 1/2$, which coincides with β for the Potts model on the Farey graph with $Q = Q_c = 2$ [11].

Figure 5 shows the r dependence of the gaps $1 - \psi_c$ and P_c . While $1 - \psi_c$ is zero for $r \leq r_c$ and finite for $r > r_c$, P_c is zero for $r \geq r_c$ and finite for $r < r_c$. These gaps play a role of an order parameter of the meta-transition. We actually find power-laws:

$$1 - \psi_c(r) \propto (r - r_c)^2 \quad \text{for } r > r_c, \quad (15)$$

$$P_c(r) \propto r_c - r \quad \text{for } r < r_c. \quad (16)$$

The power exponents 2 and 1 are numerically estimated with good precision.

In conclusion, we investigated the meta-transition in the bond-percolation on the random hierarchical small-world network whose topology can be varied by continuous parameter r . It is clearly shown that a meta-transition at r_c from iBKT transition to abrupt transition corresponds to the event that the SNBP gets over

the ordered fixed point to enter the unphysical region. The similar classification is proposed by Boettcher and Brunson [15, 16]. At the transition for $r < r_c$, which is governed by a transcritical bifurcation point, the order parameter is discontinuous and the fractal exponent is continuous. At the transition for $r > r_c$, which is governed by a saddle-node bifurcation point, the order parameter is continuous and the fractal exponent is discontinuous. At the marginal transition at $r = r_c$, which is governed by a pitchfork bifurcation point, both of the fractal exponent and the order parameter are continuous. The meta-transition is characterized by a “meta-order parameter”: the gaps of the order parameter for $r < r_c$ and the gap of the fractal exponent for $r > r_c$, both of which continuously vanish as $r \rightarrow r_c \pm 0$, respectively. Universality of the present criticality of the phase transitions, Eqs. (11, 14), and that of the meta-transition, Eqs. (15, 16), is an open question.

Continuity of ψ is noteworthy because it is related to the divergence of a correlation length ξ as $1 - \psi \propto \xi^{-1}$ in nonamenable graphs such as enhanced trees [4], which have small-world property in the sense that the dimension is proportional to $\ln N$. If we extend the concept of correlation length in general small-world systems by $\xi \propto (1 - \psi)^{-1}$, the difference between the critical-order transitions and conventional phase transitions stands out. The order parameter m is continuous and ξ^{-1} is discontinuous at an iBKT transition for $r > r_c$ and m is discontinuous and ξ^{-1} is continuous at a abrupt transition for $r < r_c$. On the other hand, both of m and ξ^{-1} are discontinuous at ordinary first order transitions and both of them are continuous at ordinary second order transitions. Furthermore, we consider that the power-law transition at the meta-transition point is not a generic critical-order transition with power-law (T1) but special one at the marginal point. This transition is governed by stable fixed point [11], and ψ is continuous therein while a power-law transition is ordinarily governed by a unstable fixed point, and ψ is discontinuous therein. Such a generic power-law transition is observed, e.g., by extending the present model; a transition occurs at the unstable NTFP shown in Fig. 3 if different open-bond probabilities are given for the backbone and shortcut edges to provide $p_0 > p_{\text{sn}}(r, p)$ (See Ref. [5]).

The Authors thank to S. Boettcher and K. Nemoto for fruitful discussions. This work was supported by Grant-in-Aid for Young Scientists (B) Grant number 24740054 and 25800214, and JST, ERATO, Kawarabayashi Large Graph Project.

* nogawa@med.toho-u.ac.jp

† hasegawa@m.tohoku.ac.jp

[1] S. N. Dorogovtsev, A. V. Goltsev, and J. F. F. Mendes,

- Rev. Mod. Phys. **80**, 1275 (2008).
- [2] T. Nogawa and T. Hasegawa, J. Phys. A: Math. Theor. **42**, 145001 (2009).
- [3] M. Hinczewski and A. N. Berker, Phys. Rev. E **73**, 066126 (2006).
- [4] T. Nogawa and T. Hasegawa, J. Phys. A: Math. Theor. **42**, 478002 (2009).
- [5] T. Hasegawa, M. Sato, and K. Nemoto, Phys. Rev. E **82**, 046101 (2010).
- [6] E. Müller-Hartmann and J. Zittartz, Phys. Rev. Lett. **33**, 893 (1974).
- [7] R. H. Schonmann, Commun. Math. Phys. **219**, 271 (2001).
- [8] S. Boettcher, V. Singh, and R. M. Ziff, Nat. Comm. **3**, 787 (2012).
- [9] T. Hasegawa and K. Nemoto, Phys. Rev. E **81**, 051105 (2010).
- [10] T. Nogawa, T. Hasegawa, and K. Nemoto, Phys. Rev. Lett. **108**, 255703 (2012).
- [11] T. Nogawa, T. Hasegawa, and K. Nemoto, Phys. Rev. E **86**, 030102(R) (2012).
- [12] Z. Zhang and F. Comellas, Theo. Comp. Sci. **412**, 865 (2011).
- [13] H. D. Rozenfeld and D. ben-Avraham, Phys. Rev. E **75**, 061102 (2007).
- [14] A. N. Berker, M. Hinczewski, and R. R. Netz, Phys. Rev. E **80**, 041118 (2009).
- [15] S. Boettcher and C. T. Brunson, Phys. Rev. E **83**, 021103 (2011).
- [16] S. Boettcher and C. T. Brunson, Front. Physiol. **2**, 102 (2011).